



UNIVERSITY OF LEEDS

This is a repository copy of *Performance Analysis of Adaptive Notch Filter Active Damping Methods for Grid-Connected Converters under a Varying Grid Impedance*.

White Rose Research Online URL for this paper:  
<http://eprints.whiterose.ac.uk/117544/>

Version: Accepted Version

---

**Proceedings Paper:**

Rufa'i, NA, Zhang, L and Chong, B (2017) Performance Analysis of Adaptive Notch Filter Active Damping Methods for Grid-Connected Converters under a Varying Grid Impedance. In: 2017 IEEE Manchester PowerTech. 12th IEEE PES PowerTech Conference, 18-22 Jun 2017, Manchester, UK. IEEE . ISBN 978-1-5090-4237-1

<https://doi.org/10.1109/PTC.2017.7981203>

---

(c) 2017, IEEE. This is an author produced version of a paper published in 2017 IEEE Manchester PowerTech. Personal use of this material is permitted. Permission from IEEE must be obtained for all other uses, in any current or future media, including reprinting/republishing this material for advertising or promotional purposes, creating new collective works, for resale or redistribution to servers or lists, or reuse of any copyrighted component of this work in other works. Uploaded in accordance with the publisher's self-archiving policy.

**Reuse**

Unless indicated otherwise, fulltext items are protected by copyright with all rights reserved. The copyright exception in section 29 of the Copyright, Designs and Patents Act 1988 allows the making of a single copy solely for the purpose of non-commercial research or private study within the limits of fair dealing. The publisher or other rights-holder may allow further reproduction and re-use of this version - refer to the White Rose Research Online record for this item. Where records identify the publisher as the copyright holder, users can verify any specific terms of use on the publisher's website.

**Takedown**

If you consider content in White Rose Research Online to be in breach of UK law, please notify us by emailing [eprints@whiterose.ac.uk](mailto:eprints@whiterose.ac.uk) including the URL of the record and the reason for the withdrawal request.



[eprints@whiterose.ac.uk](mailto:eprints@whiterose.ac.uk)  
<https://eprints.whiterose.ac.uk/>

# Performance Analysis of Adaptive Notch Filter Active Damping Methods for Grid-Connected Converters under a Varying Grid Impedance

Nabila Ahmed Rufa'I, Li Zhang and Benjamin Chong  
School of Electronic and Electrical Engineering  
University of Leeds  
United Kingdom  
e112nari@leeds.ac.uk

**Abstract**—Grid connected converters commonly use LCL filters for harmonic content suppression. However, associated with such filters is a resonant frequency at which the gain value increases significantly. To mitigate this problem, a notch filter is introduced into the current control loop of the converter. When tuned to the LCL resonant frequency, it introduces an opposing notch, thereby neutralizing the resonance effect. To ensure robustness of the control system, the notch filter must be made adaptive. This will ensure any variation in the resonant frequency, either due to a change in grid impedance or aging of components, can be tracked accurately. This paper provides two novel methods of online tuning for the adaptive notch filter using grid impedance estimation and discrete Fourier transform (DFT) techniques. Simulation results show that both methods are capable of fast and accurate detection of the resonant frequency, for varying strengths of the grid.

**Index Terms**— active damping, adaptive notch filter, DFT, grid impedance estimation.

## I. INTRODUCTION

Voltage source converter (VSC) based grid converters use medium to high frequency PWM switching schemes to synthesise the sinusoidal voltage waveform for real and reactive power exchanges with the grid. However, the resultant PWM carrier and its side-band frequencies lead to distorted current flowing into the grid, hence necessitating proper grid filtering. As opposed to a purely inductive filter, an LCL filter has proven to be advantageous, as it can provide better harmonic reduction with smaller inductor values, thereby enabling lower inverter switching frequencies to be used. However, due to the presence of a capacitor, this type of filter exhibits a unique resonant frequency. At this frequency, the LCL filter offers negligible impedance, leading to a rapid increase in gain value. This amplification of unwanted frequencies (harmonics) prevents the PI controller of the converter from accurately tracking its reference, ultimately leading to instability.

One of the simplest techniques to deal with the resonant frequency issue is passive damping, which involves the use of a resistor connected in series with the capacitor [1]-[3]. The

major disadvantage of this method is significant power losses, especially in large power applications. Furthermore, employing passive damping reduces the attenuation capacity of high frequency components.

Active damping methods have also been proposed, such as a virtual resistor, which emulates a real resistor but without the losses, by means of a current feedback [3]-[5]. Its major drawback, however, is the requirement for a differentiator, which accentuates high frequency signals [6]. Auxiliary filters such as low pass, lead-lag and notch filters have been used within the system control loop to provide filter damping in [3],[7], where the notch filter performance has proven to be the most effective [7]. In [8], proportional-resonant (PR) controllers tuned to the LCL resonant frequency are used to achieve active damping, as they are capable of selective frequency amplification [9]. Reference [10] uses an improved discrete Fourier transform (DFT) algorithm within the current control loop, known as the sliding DFT (SDFT) to determine both the magnitude and phase of the resonant frequency. Because it operates within a smaller window, the SDFT is less computationally intensive than the DFT. Its limitation, however, is that the particular value of the resonant frequency must be known beforehand. Reference [9] proposed a rather invasive method of determining the resonant frequency by grid impedance estimation via controlled excitation of the LCL filter.

It is, however, important to note that the resonant frequency is not always fixed. It may vary either due to a change in line impedance or nonlinear inductors, showing a current dependent inductance [7],[11]-[13]. A shift in filter resonant frequency causes harmonic distortions of the system voltages and currents. These harmonics have been known to affect the accuracy and performance of power system components such as transformers, measuring instruments and power transmission systems [14].

One possible method of dealing with this problem is to use several parallel controllers or filters each tuned to a specific resonant frequency as in [15]. However, this would require prior knowledge of all possible values of the resonant

frequency, making it impractical and rather expensive, especially in situations where a wide grid impedance variation is expected. For this reason, adaptive controllers have been proposed.

In [12], a digital notch filter was designed with its frequency set lower than the actual LCL filter resonant frequency, thereby increasing the system stability margin. Clearly, such a method cannot cater for wide deviations of the resonant frequency due to grid impedance changes. A discrete adaptive notch filter (ANF) has been proposed for active damping in [11], but the exact method of resonant frequency detection has not been specified. Reference [16] provides an online iterative tuning method for the ANF via modification of the damping ratios of the zeros. However, it is based on the assumption that the resonant frequency is already known. In [13], the ANF tracks the resonant frequency making use of a look-up table for LCL filter parameter values.

This paper proposes two novel methods for an ANF used as an active method of damping, where LCL filter resonance is suppressed by modifying the control algorithm. One is based on grid impedance estimation (GIE) and the other uses the DFT scheme. Both methods are lossless, easy to implement and accurate. They do not require prior knowledge of the resonant frequency, and are therefore excellent for varying frequencies. The paper describes the principles and design of these two respective methods and compares their performance.

## II. SYSTEM DESCRIPTION

The system under study is a grid connected solar PV panel with a 3-phase VSC and series connected LCL filter as shown in Fig. 1. The solar panel is modelled as a constant voltage source. The grid is represented by its Thevenin equivalent voltage,  $V_g$ , in series with the grid resistance ( $R_g$ ) and inductance ( $L_g$ ).  $R_d$  connected in series with the filter capacitor represents the passive damping resistor. Power flow from the VSC to the grid is controlled through the voltage oriented control (VOC) technique [17], which is based on independent control of active and reactive powers through conversion of 3-phase stationary quantities to the synchronous reference frame (dqo transform). The rotation of the dq-quantities is synchronised with the grid voltage through a phase locked loop (PLL) technique. Decoupled control is therefore achieved by aligning the d-axis with the grid voltage vector,  $V_d$  while the q-axis voltage becomes zero [2]. By decomposing the VSC output current components into  $i_d$  and  $i_q$ ,  $i_d$  is used to regulate the flow of active power into the system. The active and reactive powers ( $P$  and  $Q$ ) are therefore respectively given by:

$$P = \frac{3}{2} V_d i_d \quad (1)$$

and

$$Q = -\frac{3}{2} V_d i_q. \quad (2)$$

The PI current controllers are tuned based on the symmetrical optimum method [18], which approximates an LCL filter to an L-filter, since both filters have similar characteristics in the low frequency range. The block diagram for the current control loop is shown in Fig. 2.

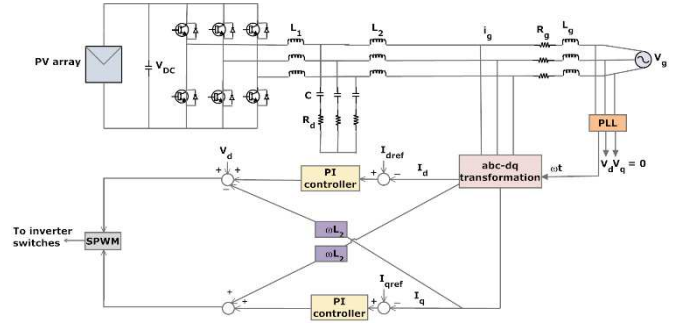


Fig. 1. Block diagram for Voltage Oriented Control of grid connected VSC with LCL filter

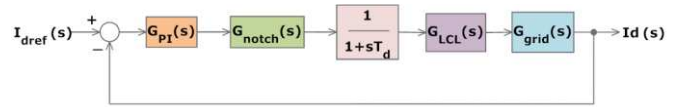


Fig. 2. Current control loop for grid connected LCL filter (d-axis)

Here:  $G_{pI}(s)$  is the PI-controller transfer function,

$G_{notch}(s)$  is the notch filter transfer function,

$T_d$  is the time delay typically associated with PWM,

$G_{LCL}(s)$  is the LCL filter transfer function and

$G_{grid}(s)$  is the grid impedance transfer function.

The notch filter is placed in the forward path of the closed loop current controller, as shown in Fig. 2. It is capable of producing very high attenuation at the resonant frequency, effectively neutralizing the effect of the LCL filter resonance. This is achieved through the introduction of a conjugate pair of complex zeros which are tuned to the resonant frequency of the LCL filter, thereby effectively cancelling out the LCL filter poles. With LCL filter parameters given as  $L_1$ ,  $L_2$  and  $C$ , the transfer function for the undamped LCL filter is:

$$G_{LCL}(s) = \frac{1}{s^3 L_1 L_2 C + s(L_1 + L_2)} \quad (3)$$

and the frequency response is shown in Fig. 3.

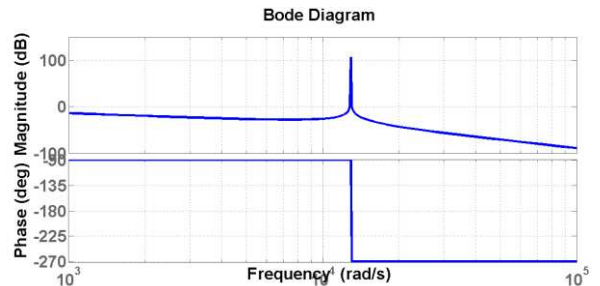


Fig. 3. Bode plot for undamped LCL filter

The notch filter transfer function is:

$$G_{notch}(s) = \frac{s^2 + 2\zeta_1 \omega_0 s + \omega_0^2}{s^2 + 2\zeta_2 \omega_0 s + \omega_0^2}, \quad (4)$$

where  $\zeta_1, \zeta_2$  are the damping ratios of the zeros and poles respectively, and  $\omega_0$  is the natural frequency of the notch filter.

In the analysis of the LCL filter, the grid inductance ( $L_g$ ) must be considered. Consequently, the resonant frequency ( $\omega_{res}$ ) is described by (5) as:

$$\omega_{res} = \sqrt{\frac{L_1 + (L_2 + L_g)}{L_1(L_2 + L_g)C}} \quad (5)$$

Changes in grid side inductance will change the resonant frequency,  $\omega_{res}$ , making the notch filter less effective. To deal with this problem, an ANF is necessary. If this can detect any variations in  $\omega_{res}$  due to grid impedance change and correspondingly retune the notch filter parameters by setting  $\omega_0$  in (4) to  $\omega_{res}$  in (5), stable operation of the grid converter can be obtained.

### III. NOTCH FILTER FREQUENCY ANALYSIS

Considering (4), if  $\omega_0$  is tuned to the LCL filter resonant frequency  $\omega_{res}$ , it becomes:

$$G_{notch}(j\omega_{res}) = \frac{(j\omega_{res})^2 + 2\zeta_1\omega_{res}(j\omega_{res}) + \omega_{res}^2}{(j\omega_{res})^2 + 2\zeta_2\omega_{res}(j\omega_{res}) + \omega_{res}^2},$$

which reduces to:

$$G_{notch}(j\omega_{res}) = \frac{\zeta_1}{\zeta_2} \quad (6)$$

Equation (6) suggests that the depth of the 'notch' is dependent on the ratio of the damping of zeros and poles respectively. As our desire is to obtain high attenuation at the resonant frequency,  $\zeta_2$  should ideally be made sufficiently higher than  $\zeta_1$ , making the gain at the resonant frequency close to 0.

From Fig. 4, it is clear that the smaller the value for  $\zeta_2$ , the shorter the depth of the notch, but the narrower the width. Consequently, the phase lag is smaller. This gives a higher system loop gain, phase margin and bandwidth. Since the notch filter zeros are responsible for cancelling the effect of the resonant poles of the LCL filter, the poles are chosen such that they lie further left into the imaginary axis [6] to prevent them from having an effect on the dynamics of the system and also to prevent possible cancellation of notch filter zeros. This causes the entire system to have a wider range of stability. To ensure that they are sufficiently damped, they lie closer to the real axis (close to unity). Hence,  $\zeta_2$  is taken to be 1.  $\zeta_1$  is taken as a 100 times smaller (0.01), since a larger value would reduce the sharpness of the notch.

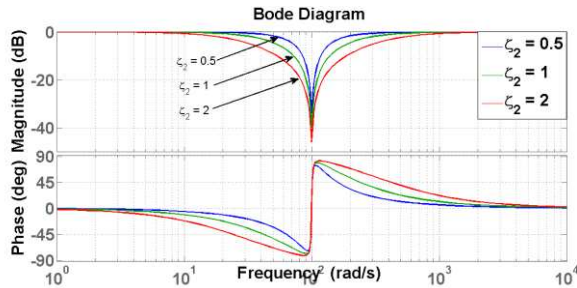


Fig. 4. Notch filter bode plot showing the effect of increasing  $\zeta_2$

### IV. GRID IMPEDANCE ESTIMATION (GIE) METHOD

This method involves real time estimation of the complex grid impedance by measurement of the fundamental components of the voltage and current at the point of common coupling (PCC). The estimates can then be used to tune the ANF, which is used for active damping of the LCL filter as shown in Fig. 5. As the measured fundamental voltage and current components may be affected by the resonance effect, they must be extracted using some form of filter, which in this case is a band pass filter (BPF) centred at 50 Hz. The usual compromise between speed of response and rejection of noise apply in choosing the filter bandwidth. The new impedance is used to set the new value for the natural frequency of the ANF according to (5).

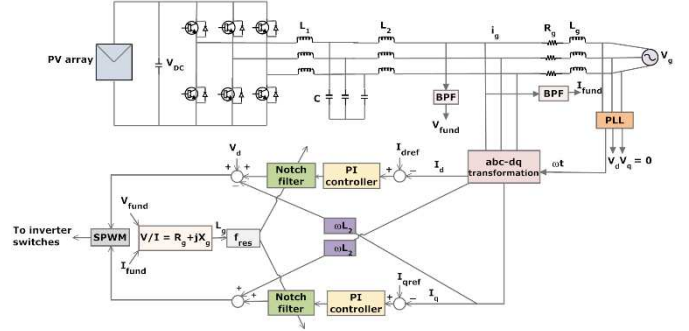


Fig. 5. Voltage Oriented Control of grid connected VSC with adaptive notch filters (GIE method)

### V. DISCRETE FOURIER TRANSFORM (DFT) METHOD

The spectrum at the output of the VSC contains a very wide range of frequencies formed from combinations of the system (i.e. grid) frequency and the converter switching frequency. Some of these will lie near the filter resonance and hence will be amplified; the resulting practical problem is perturbation of the control system. Estimation of the resonance frequency is not the main aim per se, but rather reduction of the most deleterious frequency components. It follows that an alternative approach to the resonance problem is to seek out the largest frequency component and apply a notch to it.

This second method therefore involves adapting the parameters of the notch filter using a spectral measurement of the filter output, which is conveniently performed using a discrete Fourier transform (DFT) filter. Naturally, a fast Fourier transform (FFT) is actually used for computational efficiency and yields the magnitudes of the frequencies present within the signal as shown in Fig. 6. The harmonic grid current is first passed through the DFT filter, which separates it into the corresponding frequency bands, from which the resonant frequency can easily be identified. When no grid resistance is considered, the system is completely undamped and the resonant frequency is the highest frequency of the signal. However, in the case of a distribution system, the effect of grid resistance cannot be ignored, owing to its intrinsic damping. Depending on the magnitude of this resistance, the resonant frequency may become the second highest frequency in the signal, after the fundamental frequency. This will therefore hinder the resonant frequency tracking. As a solution, a high pass filter (HPF) is used at the LCL filter output. This ensures

the resonant frequency is the largest frequency component and it is used to retune the ANF parameters accordingly.

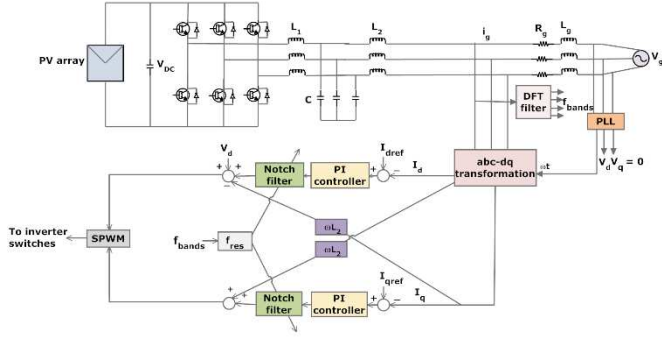


Fig. 6. Voltage Oriented Control of grid connected VSC with adaptive notch filters (DFT method)

For  $n$  frequency components, the DFT of a signal is defined as:

$$F[n] = \sum_{k=0}^{N-1} f[k] e^{-j \frac{2\pi nk}{N}}, \quad (7)$$

where  $N$  is the total number of samples in the signal and  $f[k]$  is the  $k$ th time domain sample of the time series.

The frequency resolution (FR) of the DFT, defined as its ability to resolve two adjacent frequencies, is given as:

$$FR = \frac{f_s}{N}, \quad (8)$$

where  $f_s$  is the sampling frequency, which is chosen based on the Nyquist criterion.

Obviously, both the FFT window size and the sampling frequency influences frequency resolution. To improve FR, either  $N$  can be increased or  $f_s$  can be made smaller. However, this will be at the expense of increased computation time ( $t$ ), as shown in (9) below:

$$t = N \times T_s. \quad (9)$$

Upon finding the DFT, the corresponding frequency,  $f$  will be:

$$f = \frac{f_s}{N} \times n, \quad (10)$$

where  $n$  is the frequency bin number.

In practice, because the converter output spectrum is fairly flat, the frequency at the maximum value of  $|F(n)|$  approximates well to the actual LCL resonant frequency.

## VI. SIMULATION RESULTS

All simulations have been carried out using MATLAB/Simulink software. The frequency range for the notch filter is chosen based on (5), with  $L_g$  varying from 0 to infinity. This corresponds to a range of 240 Hz to 2.06 kHz. Table I specifies the system parameters used in the simulation.

Table I  
System parameters

| Parameter                        | Rating                         |
|----------------------------------|--------------------------------|
| Converter Rated Power (P)        | 100 kW                         |
| Grid frequency (f)               | 50 Hz                          |
| $L_1/C/L_2$                      | 5 mH/88.4 $\mu$ F/68.8 $\mu$ H |
| Resonant frequency ( $f_{res}$ ) | 2.06 kHz (13 krad/s)           |
| Grid Impedance ( $R_g/L_g$ )     | 0.5 $\Omega$ /1 mH             |
| Sampling frequency ( $f_s$ )     | 4.1 kHz                        |

### A. GIE Method

The band pass filter frequency response is shown in Fig. 7. The first stop band is chosen to be 45 Hz, and the last 60 Hz with a pass band lying between 50-55 Hz. This setting extracts the fundamental signals for the PCC measurements in 0.28 seconds.

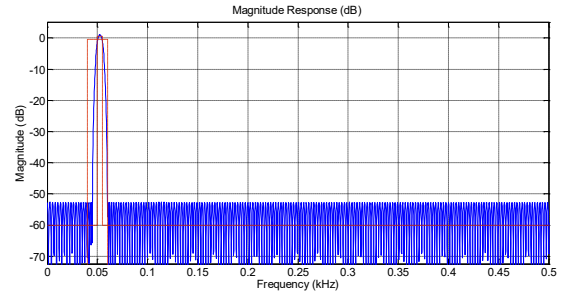
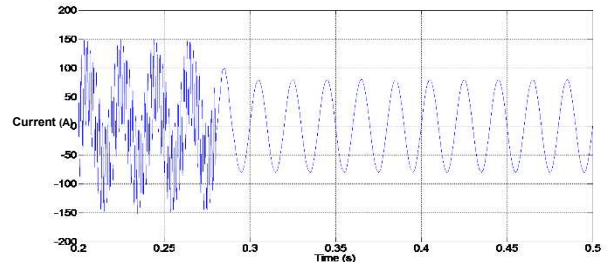
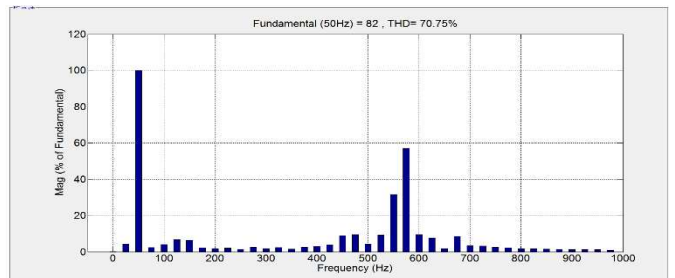


Fig. 7. Frequency response for band pass filter

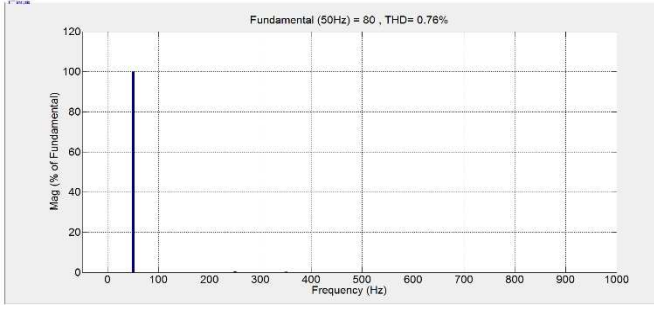
Using the parameters in table I, the notch filter is unable to track the new resonant frequency, when grid impedance is introduced. This leads to a very large THD of 70.75% (Fig. 8 (a) and (b)). Once the ANF is turned on at 0.28s, it determines the new resonant frequency, tuning the notch filter accordingly. This reduces the THD to 0.76% (Fig. 8 (a) and (c)). The grid inductance of 1 mH is accurately estimated at 0.28 seconds, as shown in Fig. 9.



(a) d-axis grid current



(b) Harmonic spectrum before 0.28s



(c) Harmonic spectrum after 0.28s  
Fig. 8. LCL and grid impedance with ANF turned on at 0.28s

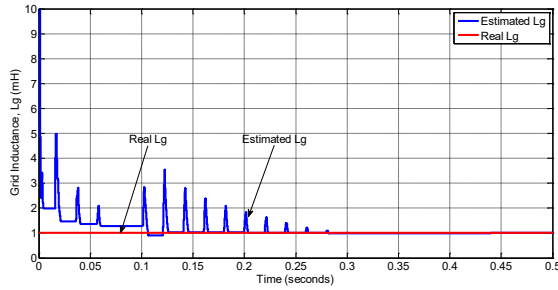


Fig. 9. Lg estimation based on GIE

Table II shows the resonant frequency estimation based on the GIE method for varying strengths of the grid. It is apparent that the lower the short circuit ratio (SCR) of the grid, the higher the X/R ratio and hence the weaker the network. This, however, does not affect the quality of the waveforms as the total harmonic distortion (THD) values are all less than 1%. Hence, the GIE method is capable of dealing with any form of grid, irrespective of strength.

Table II  
Resonant frequency detection based on GIE method

| $L_g$<br>(mH) | SCR  | X/R<br>ratio | Actual<br>$f_{res}$ (Hz) | Estimated<br>$f_{res}$ (Hz) | THD<br>(%) |
|---------------|------|--------------|--------------------------|-----------------------------|------------|
| 1             | 6.1  | 0.63         | 570.4                    | 569.5                       | 0.76       |
| 2             | 4.5  | 1.26         | 442.5                    | 442.8                       | 0.49       |
| 3             | 3.4  | 1.90         | 388.2                    | 389.6                       | 0.58       |
| 4             | 2.65 | 2.52         | 357.4                    | 356.7                       | 0.79       |
| 5             | 2.18 | 3.14         | 337.4                    | 336.9                       | 0.77       |

## B. DFT Method

In order to prevent the fundamental frequency from affecting the accuracy of resonant frequency tracking, HPF is used to remove all frequencies below 100 Hz. The filter response is shown in Fig. 10.

The DFT is taken as an 8192-point FFT ( $2^{13}$ ). With a sampling frequency of 10 kHz, the FR according to (8) is:

$$FR = \frac{10000}{8192} = 1.22$$

The computational time (t) therefore becomes:

$$t = 8192 \times 1 \times 10^{-4} = 0.82 \text{ s}$$

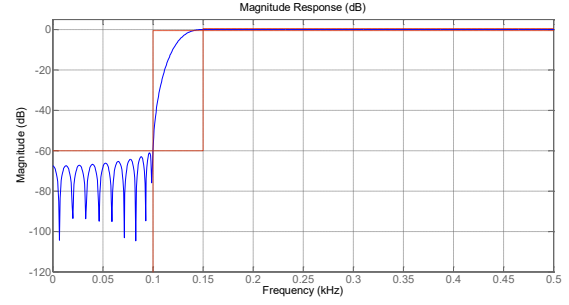
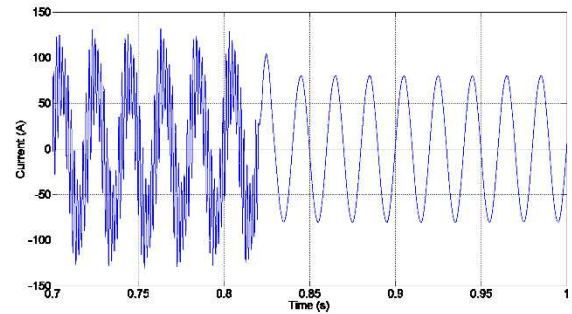
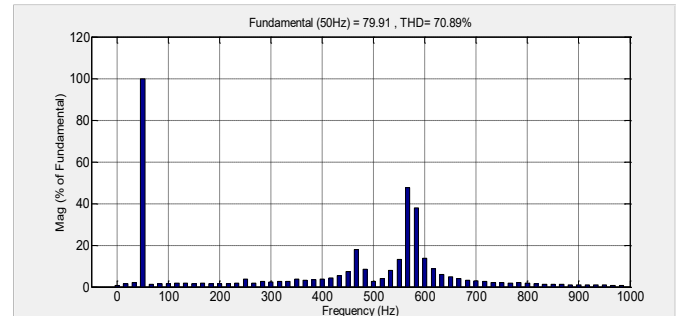


Fig. 10. Frequency response for high pass filter

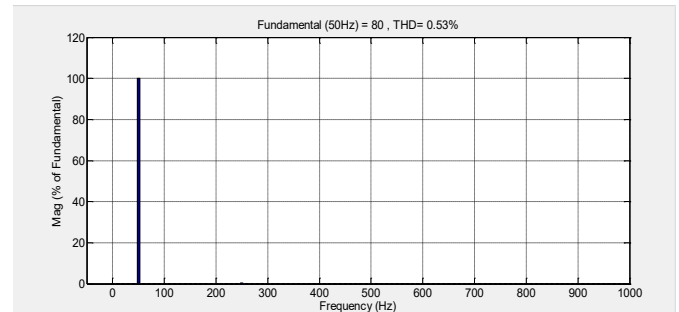
Fig. 11 show the performance of the DFT method when the grid impedance is introduced. The notch filter is unable to track the new resonant frequency of 570.4 Hz, leading to a THD of 70.89% as shown in Fig. 11 (a) and (b). Once the ANF is turned on at 0.82s, it determines the new resonant frequency as 573.7 Hz, tuning the notch filter accordingly. This reduces the THD to 0.53% as in Fig. 11 (a) and (c). Fig. 11 (d) shows the spectral power corresponding to the new resonant frequency.



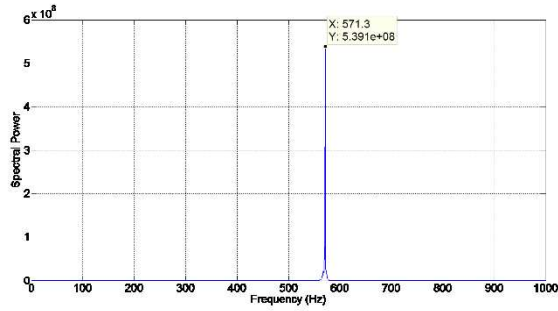
(a) d-axis grid current



(b) Harmonic spectrum before 0.82 s



(c) Harmonic spectrum after 0.82 s



(d) Resonant frequency detection

Fig. 11. LCL and grid impedance with ANF turned on at 0.82 s

Table III summarizes the frequencies detected by the DFT method.

Table III  
Resonant frequency detection based on DFT method

| $L_g$<br>(mH) | SCR  | X/R<br>ratio | Actual<br>$f_{res}$ (Hz) | Estimated<br>$f_{res}$ (Hz) | THD<br>(%) |
|---------------|------|--------------|--------------------------|-----------------------------|------------|
| 1             | 6.1  | 0.63         | 570.4                    | 573.7                       | 0.53       |
| 2             | 4.5  | 1.26         | 442.5                    | 441.9                       | 0.57       |
| 3             | 3.4  | 1.90         | 388.2                    | 388.2                       | 0.77       |
| 4             | 2.65 | 2.52         | 357.4                    | 361.3                       | 0.94       |
| 5             | 2.18 | 3.14         | 337.4                    | 336.9                       | 0.72       |

The table above shows that a THD of  $< 1\%$  is also obtained when the notch filter is tuned according to the resonant frequency from the DFT filter, for all strengths of the grid.

## VII. COMPARISON BETWEEN THE METHODS

Fig. 12 compares the actual resonant frequencies with those determined from the GIE and DFT methods. For both, there is a good agreement between the estimates and the actual values, with the GIE method being slightly more accurate than the DFT method.

In terms of computation time, the GIE method is almost three times faster than the DFT method, taking only 0.28 s to determine the grid inductance. Furthermore, unlike the DFT method, it is not affected by grid resistance. It is, however, not without drawbacks. Firstly, it requires a sensor and filter each for the measured grid voltage and current. On the other hand, the DFT method needs only one sensor and one filter for the grid current. Also, due to its dependence on Ohms law, frequency detection in the GIE method is impossible without information on the grid resistance. The DFT method, however, does not require prior knowledge of the grid.

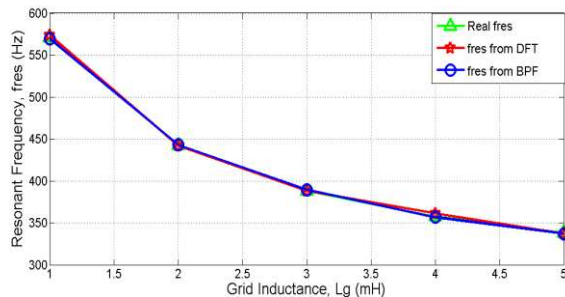


Fig. 12. Comparison between real and estimated resonant frequencies (DFT and GIE methods)

In conclusion, the GIE method seems to be the best method for networks where grid resistance information is readily available. If such information is not present, the DFT method would be the better choice, especially in the case of high voltage (HV) systems, where grid resistance is negligible [19].

## REFERENCES

- [1] K. Abd El Wahid Hamza, H. Linda, and L. Cherif, "LCL filter design with passive damping for photovoltaic grid connected systems," in *Renewable Energy Congress (IREC), 2015 6th International*, 2015, pp. 1-4.
- [2] R. Teodorescu, M. Liserre, and P. Rodriguez, *Grid converters for photovoltaic and wind power systems* vol. 29: John Wiley & Sons, 2011.
- [3] C. Zhang, T. Dragicevic, J. C. Vasquez, and J. M. Guerrero, "Resonance damping techniques for grid-connected voltage source converters with LCL filters—A review," in *Energy Conference (ENERGYCON), 2014 IEEE International*, 2014, pp. 169-176.
- [4] W. Zhao and G. Chen, "Comparison of active and passive damping methods for application in high power active power filter with LCL-filter," in *Sustainable Power Generation and Supply, 2009. SUPERGEN'09. International Conference on*, 2009, pp. 1-6.
- [5] K. Wessels, J. Dannehl, and F. W. Fuchs, "Active damping of LCL-filter resonance based on virtual resistor for PWM rectifiers—Stability analysis with different filter parameters," in *2008 IEEE Power Electronics Specialists Conference*, 2008, pp. 3532-3538.
- [6] F. Bronchart, Y. Mollet, and J. Gyselinck, "LCL filters for a grid emulator application-Comparative study of active damping techniques," in *Industrial Electronics Society, IECON 2013-39th Annual Conference of the IEEE*, 2013, pp. 2087-2092.
- [7] J. Dannehl, M. Liserre, and F. W. Fuchs, "Filter-based active damping of voltage source converters with filter," *IEEE Transactions on Industrial Electronics*, vol. 58, pp. 3623-3633, 2011.
- [8] N. Zhang, H. Tang, and C. Yao, "A systematic method for designing a PR controller and active damping of the LCL filter for single-phase grid-connected PV inverters," *Energies*, vol. 7, pp. 3934-3954, 2014.
- [9] M. Liserre, F. Blaabjerg, and R. Teodorescu, "Grid impedance detection via excitation of LCL-filter resonance," in *Fourtieth IAS Annual Meeting. Conference Record of the 2005 Industry Applications Conference, 2005.*, 2005, pp. 910-916.
- [10] J.-s. Lee, D.-H. Kang, H.-G. Jeong, and K.-B. Lee, "Active damping for large-scale wind power systems with an LCL-filter using an improved DFT," in *IECON 2011-37th Annual Conference on IEEE Industrial Electronics Society*, 2011, pp. 1179-1184.
- [11] M. Ciobotaru, A. Rossé, L. Bede, B. Karanayil, and V. G. Agelidis, "Adaptive notch filter based active damping for power converters using LCL filters," in *Power Electronics for Distributed Generation Systems (PEDG), 2016 IEEE 7th International Symposium on*, 2016, pp. 1-7.
- [12] W. Yao, Y. Yang, X. Zhang, and F. Blaabjerg, "Digital notch filter based active damping for LCL filters," in *Applied Power Electronics Conference and Exposition (APEC), 2015 IEEE*, 2015, pp. 2399-2406.
- [13] Y.-C. Cho, K.-Y. Choi, and R.-Y. Kim, "Adaptive damping scheme of LCL filter resonance under inductance variation for a single-phase grid-connected inverter," in *2015 9th International Conference on Power Electronics and ECCE Asia (ICPE-ECCE Asia)*, 2015, pp. 978-983.
- [14] S. Chattopadhyay, M. Mitra, and S. Sengupta, "Electric power quality," in *Electric Power Quality*, ed: Springer, 2011, pp. 5-12.
- [15] M. V. Mane and M. A. Agashe, "An adaptive notch filter for noise reduction and signal decomposition," *IJCSI*, 2011.
- [16] T.-I. Kim, W. Bahn, J.-M. Yoon, J.-S. Han, J.-H. Park, S.-S. Lee, et al., "Online tuning method for notch filter depth in industrial servo systems," in *Control Conference (CCC), 2016 35th Chinese*, 2016, pp. 9514-9518.
- [17] M. Zarif and M. Monfared, "Step-by-step design and tuning of VOC control loops for grid connected rectifiers," *International Journal of Electrical Power & Energy Systems*, vol. 64, pp. 708-713, 2015.
- [18] B. Terzić, G. Majić, and A. Slutej, "Stability analysis of three-phase PWM converter with LCL filter by means of nonlinear model," *AUTOMATIKA: časopis za automatiku, mjerenje, elektroniku, računarstvo i komunikacije*, vol. 51, pp. 221-232, 2010.
- [19] B. Fox, *Wind power integration: connection and system operational aspects* vol. 50: IET, 2007.